

Towards Efficient CR-NOMA Backscatter IoT: A DRL-driven Approach Under Practical Non-Linear Energy Harvesting

Muhammad Danish Khattak*, Muhammad Ayaan Qasmi*, Yousuf Rehan*,
Syed Asad Ullah*, Kapal Dev†, Haejoon Jung† Syed Ali Hassan*,

*School of Electrical Engineering & Computer Science (SEECS),

National University of Sciences & Technology (NUST), Islamabad, Pakistan

†Department of Electronic Engineering, Kyung Hee University (KHU), South Korea

‡CONNECT Centre and Department of Computer Science, Munster Technological University, Ireland

Emails: *{mkhattak.bee22seecs, mqasmi.bese22seecs, yrehan.bese22seecs, sullah.phdee21seecs, ali.hassan}@seecs.edu.pk

†haejoonjung@khu.ac.kr, †kapal.dev@ieee.org

Abstract—The proliferation of low-powered devices in the Internet of things (IoT) necessitates energy-efficient communication paradigms. Backscatter communication (BackCom) combined with cognitive radio-inspired non-orthogonal multiple access (CR-NOMA) offers a promising solution. However, optimizing such systems is complex, especially when considering realistic energy harvesting (EH) models. This paper investigates the sum rate optimization of an EH-enabled passive backscatter node (BN) coexisting with primary devices (PDs) in a CR-NOMA network, employing a practical non-linear EH model. We leverage deep reinforcement learning (DRL) to dynamically optimize the BN’s reflection coefficient. Crucially, We conduct a comparative study of several DRL algorithms. These include deep deterministic policy gradient (DDPG), its prioritized replay variants (PER-DDPG and CER-DDPG), and the stability-enhanced twin delayed DDPG (TD3). We also evaluate on-policy methods such as proximal policy optimization (PPO), as well as entropy-regularized algorithms like soft actor-critic (SAC) and its recurrent extension (RSAC). Additionally, we include the asynchronous advantage actor-critic (A3C) for comparison. We evaluate their performance in terms of sum rate, reflection coefficient adaptation, and harvested energy, contrasting results under non-linear versus linear EH models. Our findings provide insights into algorithm suitability for optimizing BackCom systems under realistic EH constraints, highlighting performance trade-offs and the impact of EH non-linearity.

Index Terms—Backscatter communication (BackCom), non-orthogonal multiple access (NOMA), cognitive radio (CR), deep reinforcement learning (DRL), non-linear energy harvesting (EH).

I. INTRODUCTION

The Internet of things (IoT) paradigm is driving an unprecedented surge in connected devices, many of which are resource-constrained, particularly in terms of power [1]. Addressing the energy needs of these devices sustainably is paramount. Traditional battery power faces limitations due to replacement costs and environmental impact [2]. Energy harvesting (EH) from ambient sources, such as radio frequency (RF) signals, offers a viable alternative. Backscatter commu-

nication (BackCom) emerges as a key enabling technology, allowing devices (backscatter nodes or BNs) to communicate by reflecting existing RF signals rather than generating their own, drastically reducing power consumption [3].

To accommodate the massive connectivity demands within limited spectral resources, cognitive radio-inspired non-orthogonal multiple access (CR-NOMA) provides an efficient solution. CR-NOMA allows unlicensed secondary users (like BNs) to opportunistically share the spectrum licensed to primary devices (PDs), provided the PDs quality of service (QoS) is maintained. Combining BackCom with CR-NOMA creates a spectrally and energy-efficient framework for low-power IoT networks [4], [5].

Optimizing resource allocation, such as the BN’s reflection coefficient, is crucial for maximizing performance in such systems. The reflection coefficient determines the trade-off between reflecting the signal for communication and harvesting energy from it. Due to the dynamic nature of wireless channels and energy states, traditional optimization methods often fall short. Deep reinforcement learning (DRL) has shown promise in handling such complex, sequential decision-making problems in wireless communications [6].

Traditional studies on BackCom and CR-NOMA often employ linear EH models, assuming ideal energy conversion and storage. However, real-world EH devices exhibit nonlinear characteristics, such as saturation effects, which these models overlook. For instance, Babaei et al. (2020) investigated the bit error rate (BER) performance in full-duplex CR networks using linear EH models, potentially overestimating system performance [9]. In contrast, Wang et al. (2017) proposed a multi-objective resource allocation framework for NOMA-enabled CR networks, utilizing a nonlinear EH model, leading to more accurate performance predictions and better system optimization [10]. The application of deep reinforcement learning (DRL) in BackCom systems has gained traction for

optimizing resource allocation and transmission strategies. Nie et al. (2020) employed DRL to design unmanned aerial vehicle (UAV) trajectories for BackCom systems, achieving significant energy efficiency improvements [11]. Similarly, Tran et al. (2018) utilized double deep Q-networks (DDQN) for time scheduling in RF-powered BackCom CR networks, demonstrating enhanced throughput compared to traditional methods [12].

Nevertheless, many studies in this domain neglect the complexities introduced by non-linear EH models and advanced DRL techniques, which are crucial for realistic system modeling and optimization. This paper addresses these gaps by investigating the sum rate maximization problem for a BN in a CR-NOMA BackCom network using a realistic non-linear EH model, as proposed in [8]. We formulate the problem within a DRL framework and conduct a comparative analysis of a set of state-of-the-art DRL algorithms: deep deterministic policy gradient (DDPG), prioritized experience replay DDPG (PER-DDPG), composite experience replay DDPG (CER-DDPG), twin delayed DDPG (TD3), proximal policy optimization (PPO), soft actor-critic (SAC), recurrent soft actor-critic (RSAC), and asynchronous advantage actor-critic (A3C). The key contributions of this paper are outlined as follows

- We formulate the long-term sum rate maximization problem for an EH-enabled BN in a CR-NOMA-assisted BackCom network, using a practical non-linear EH model.
- We implement and compare the effectiveness of a set of state-of-the-art DRL algorithms with various system configurations.
- We conduct extensive simulations comparing the performance of these algorithms in terms of convergence, sum rate, and harvested energy under dynamic settings.

The rest of the paper is organized as follows: Section II details the system model. Section III details the problem formulation. Section IV describes the DRL framework and the algorithms investigated. Section V presents the simulation setup and discusses the results. Section VI concludes the paper.

II. SYSTEM MODEL

We consider an uplink CR-NOMA-assisted backscatter communication scenario. The network comprises m PDs, a backscatter reader (BR, acting as a base station), and an EH-enabled BN tasked with sensing operations. Unlike conventional active transmission, the BN reflects ambient RF signals emitted by PDs, modulating its data on those signals. Each PD employs a time-division multiple access (TDMA) scheme, dividing the transmission into M time slots, each of duration $T = 1$ second. Let the channel gains between the BN and the BR be represented by h_0 , the channel gains between the m -th PD and the BR by h_m , and the channel gains between the m -th PD and the BN by $h_{m,0}$. All communication links are assumed to undergo Rayleigh fading.

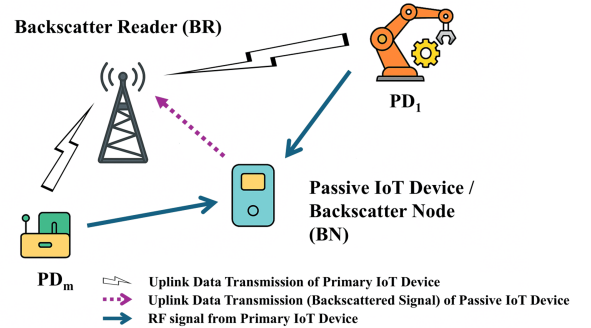


Fig. 1: System model for CR-NOMA-enabled uplink BackCom.

During each transmission slot assigned to a PD, the BN determines the proportion of incident RF power to reflect (for communication) and harvest (for energy), controlled by the reflection coefficient $\Gamma \in [0, 1]$. At $\Gamma = 0$, only energy is harvested with no data transmission, while $\Gamma = 1$ yields maximum sum rate but zero energy is harvested. Intermediate values of Γ enable a trade-off between the two. Thus, the sum rate of the BN observed at the BR in the presence of the m -th PD transmitting is expressed as

$$R_{0,m} = \log_2 \left(1 + \frac{\Gamma P_m |h_0|^2}{P_m |h_m|^2 + n_0} \right), \quad (1)$$

where P_m denotes the transmit power of the m -th PD, and n_0 is the noise power.

For EH, we have implemented and compared two different models: a practical non-linear EH model and a simpler linear EH model. The non-linear EH model, as proposed in [8], describes the harvested energy by the BN from the ambient RF signals as follows

$$\mathcal{E}_{\text{Prac}} = \frac{\theta (e^{\alpha P_m |h_{m,0}|^2} - 1)}{e^{\alpha P_m |h_{m,0}|^2} + e^{\alpha \beta}}, \quad (2)$$

where θ represents the maximum harvested energy under saturation conditions, and α and β denote parameters determined by the EH circuitry. The simpler linear EH model, widely used in literature [7], is given by

$$\mathcal{E}_{\text{Linear}} = T \eta P_m |h_{m,0}|^2, \quad (3)$$

where η is the EH efficiency coefficient and T is the time duration. In this paper, we compare these two EH models extensively to highlight the implications of employing realistic non-linear EH characteristics.

III. PROBLEM FORMULATION

In this section, we introduce a mathematical framework for formulating the sum-rate maximization problem addressed in this paper, which is subsequently solved using DRL methods. Before initiating communication, we assume that: (i) the BN has full knowledge of the channel state information (CSI) from

all primary devices, and (ii) the BN battery initially possesses adequate energy for operation. Thus, the available energy in the battery of the BN at the start of time slot t , indicated as E_t , must fulfill

$$E_t \geq \gamma T, \quad (4)$$

where γ represents the BN's energy consumption for sensing activities, with $\gamma \in [0.01, 0.1]$. The battery level at the beginning of the subsequent time slot, i.e., E_{t+1} is given by

$$E_{t+1} = \min \{E_c - \gamma T + E_t, E_c\}, \quad (5)$$

where E_c is the BN's battery capacity limit, and \mathcal{E}_x denotes the harvested energy, with $x \in \{\text{Prac, Linear}\}$. The primary objective is to optimize the BN's achievable sum-rate, denoted by $R_{0,m}$, subject to the QoS constraints of the neighbouring PDs. Hence, the optimization problem is formulated as follows

$$\max_{\Gamma} \mathbb{E} \left[\sum_{t=1}^M \zeta^{t-1} R_{0,m}(\Gamma) \right], \quad (6a)$$

$$\text{s.t. } E_{t+1} = \min \{E_c, E_t + \mathcal{E}_x - \gamma T\}, \quad (6b)$$

$$R_m \geq \log_2 \left(1 + \frac{P_m |h_m|^2}{n_0} \right), \quad \forall m, \quad (6c)$$

$$\gamma T - E_t \leq 0, \quad (6d)$$

$$0 \leq \Gamma \leq 1, \quad (6e)$$

where ζ indicates the discount factor prioritizing immediate rewards.

The optimization problem in (6) is non-convex and challenging. To handle this, we employ primal decomposition to decompose (6) into two sub-problems: an upper-layer problem solved by DRL and a lower-layer problem solved analytically. We introduce an auxiliary variable \hat{E}_t , as the net harvested energy at time slot t , computed as the difference between the total harvested energy \mathcal{E}_x and the energy γT consumed by the BN for sensing operations. Mathematically, it is expressed as

$$\hat{E}_t = \mathcal{E}_x - \gamma T, \quad (7)$$

the upper-layer optimization problem is defined as

$$\max_{\hat{E}_t} \mathbb{E} \left[\sum_{t=1}^{\infty} \zeta^{t-1} R_{0,m}(\hat{E}_t, \Gamma_t) \right], \quad (8a)$$

$$\text{s.t. } E_{t+1} = \min \{E_t + \hat{E}_t, E_c\}, \quad \forall t \quad (8b)$$

where $R_{0,m}(\hat{E}_t, \Gamma_t)$ is the optimal sum-rate solution of the lower-layer problem for a given \hat{E}_t . For a fixed \hat{E}_t , the lower-layer optimization problem is defined as

$$\max_{\Gamma_t} R_{0,m}(\Gamma_t), \quad (9a)$$

$$\text{s.t. } \gamma T - E_t \leq 0, \quad \forall t, \quad (9b)$$

$$0 \leq \Gamma_t \leq 1, \quad \forall t, \quad (9c)$$

$$\hat{E}_t \leq \mathcal{E}_x - \gamma T, \quad \forall t. \quad (9d)$$

IV. DRL IMPLEMENTATION AND ALGORITHMS

We formulate the optimization problem (8) as a markov decision process (MDP) and employ DRL to find the optimal policy $\pi(a_t | s_t)$.

A. State, Action, and Reward

1) *State Space (s_t)*: The state observed by the agent at time t includes the BN's battery energy level and the relevant channel gains. The state is represented as

$$s_t = [E_t, |h_0|^2, |h_m|^2, |h_{m,0}|^2]^T. \quad (10)$$

2) *Action Space (a_t)*: The chosen action is the reflection coefficient set by the BN at each time slot

$$a_t = \Gamma_t, \quad \Gamma_t \in [0, 1]. \quad (11)$$

Due to the continuous nature of this action space, we implement DRL algorithms that are suitable for continuous action optimization.

3) *Reward (r_t)*: The immediate reward received at time slot t corresponds to the BN's achievable sum rate during that slot

$$r_t = R_{0,m}(\Gamma_t). \quad (12)$$

B. Investigated DRL Algorithms

We implement and compare the following DRL algorithms capable of handling continuous action spaces

1) *DDPG*: An off-policy actor-critic algorithm using deep function approximators for deterministic policies. It utilizes a replay buffer and target networks for stability. It determines optimal actions a in states s by maximizing the action-value function $Q(s, a)$ as $a^*(s) = \arg \max_a Q(s, a)$. Our implementation employs neural networks with separate learning rates and adam optimization.

2) *PER-DDPG*: The PER algorithm enhances DDPG's performance through prioritized sampling of experiences based on temporal difference (TD) errors. The prioritization mechanism assigns higher sampling probabilities to experiences with larger TD errors, facilitating more efficient learning from significant state transitions.

3) *CER-DDPG*: This algorithm extends the prioritization concept by incorporating both TD-error and reward information in its sampling strategy. This approach positions it as a delicate balance between actor and critic learning.

4) *TD3*: This algorithm addresses Q-value overestimation bias through twin critic networks and delayed policy updates. Our implementation maintains a fixed update interval of 2 steps for the actor network while continuously updating the critics. The algorithm employs a replay buffer of $1M$ experiences and uses separate optimization rates for actor and critic networks. The twin critics minimize overestimation by taking the minimum of their predicted Q-values during target value computation.

5) *PPO*: An on-policy actor-critic algorithm known for its stability and ease of implementation. PPO maximizes expected cumulative rewards through iterative policy updates while maintaining proximity to the previous policy. Our implementation features a dual network architecture and uses clipped surrogate objectives to limit policy updates.

6) *SAC*: This algorithm combines off-policy actor-critic training with a maximum entropy framework, optimizing policies to maximize both expected return and entropy. It uses two Q-functions to mitigate overestimation bias and automatically tunes the temperature parameter to achieve a target entropy. The entropy regularization helps maintain exploration throughout training, which is beneficial for discovering efficient reflection strategies across varying channel conditions.

7) *RSAC*: A recurrent extension of SAC designed to handle partially observable environments by incorporating recurrent neural networks (RNNs) into the policy and value functions. RSAC enables agents to maintain a memory of past observations, improving performance in tasks where the full state is not directly observable.

8) *A3C*: This algorithm utilizes parallel actor-learners (4 workers in our implementation) operating asynchronously on separate environment instances. Each worker computes gradients using n-step returns ($n = 5$) and accumulates them asynchronously into the global networks. The parallel architecture accelerates training by gathering diverse experiences simultaneously, while the n-step returns help capture the longer-term impacts of reflection coefficient choices on both sum rate and energy availability.

Each algorithm uses neural networks to approximate the policy (actor) and/or value functions (critic).

V. SIMULATION RESULTS

A. Simulation Environment Setup

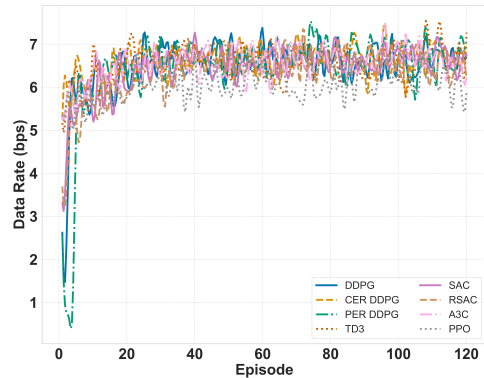
The network configuration situates the BS at the origin with an omnidirectional antenna, while the BN is at $(1m, 1m)$. In scenarios with two primary devices ($m = 2$), they're positioned at $(0m, 1m)$ and $(0m, 1000m)$. For more than two users, they're uniformly distributed between $(0m, 1m)$ and $(0m, 1000m)$ on the plane. Table I lists the overall simulation parameters.

B. Results Analysis

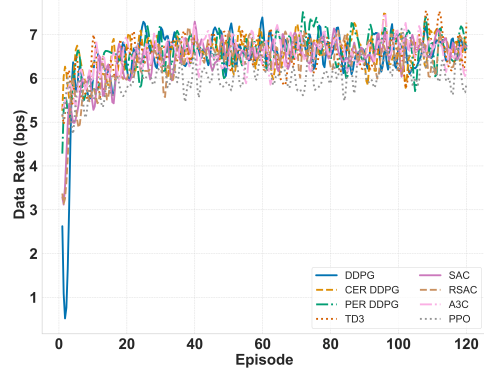
1) *Data Rate Analysis*: Fig. 2 presents the episodic data rate performance of DRL algorithms for linear and non-linear EH models. We observe that the overall episodic reward with the non-linear EH model is very similar to the non-linear EH model. This is because the data rate reward is contingent on having sufficient battery energy for transmission, not the instantaneous harvested energy amount. While the EH models differ in battery replenishment dynamics, the agents learn adaptive transmission policies to manage battery levels effectively in both scenarios. This adaptability allows them to achieve

TABLE I: Simulation Parameters

Parameter Description	Symbol	Value
Time Slot Duration	T	1 sec
Carrier Frequency	f_c	914 MHz
Bandwidth	W	10 MHz
Noise Power	σ^2	-170 dBm
Path Loss Exponent	α	3
Maximum Battery Capacity	E_c	0.2 J
Maximum Transmit Power	P_m	20 dBm
Max Harvested Power	θ	0.02 W
Circuit Parameter	α	6400
Circuit Parameter	β	0.003
Efficiency Coefficient	η	0.7
Discount Factor	ζ	0.99
Actor Learning Rate	λ_a	0.001
Critic Learning Rate	λ_c	0.004
Replay Buffer Size	K	10,000
Batch Size	S	32
Soft Update Parameter	ξ	0.01



(a) Linear EH model.



(b) Non-linear EH model

Fig. 2: Data rate performance per episode under (a) linear and (b) non-linear EH models.

comparable cumulative data rates. Both models demonstrate rapid convergence and stable long-term performance. However, subtle variations indicate the adaptability differences among algorithms to distinct EH characteristics.

The comparative analysis in Fig. 3 further substantiates these observations by showcasing the averaged episodic data rate across linear and non-linear models. It confirms that algorithmic performance is robust against EH model variations.

2) *EH Analysis*: Fig. 4 presents the harvested energy performance for the evaluated RL agents. Under the linear EH model

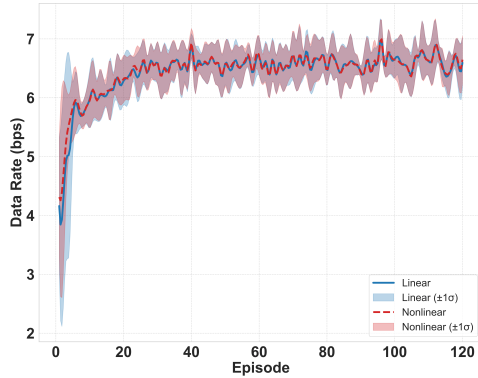


Fig. 3: Average episodic data rate comparison (linear versus non-linear EH).

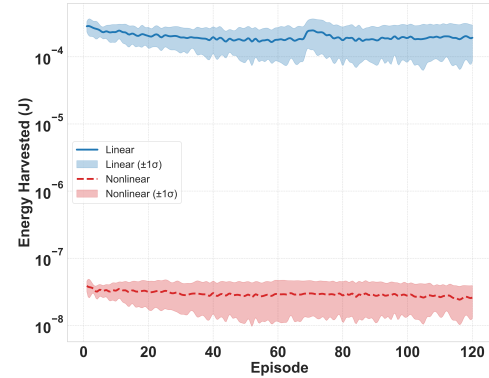
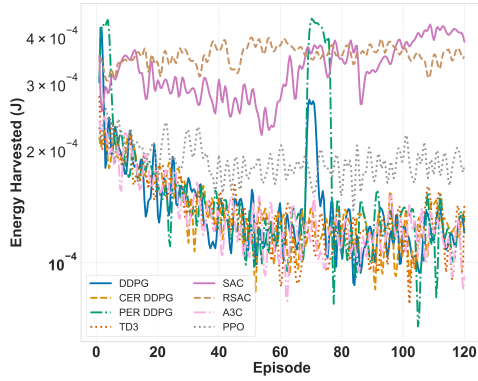
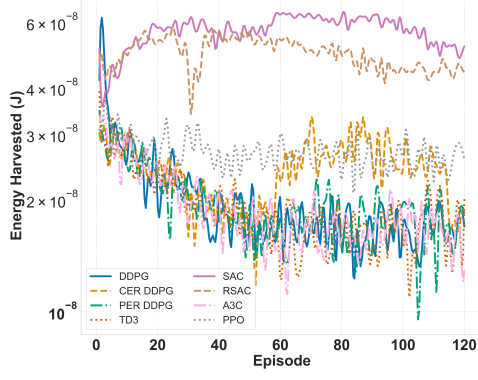


Fig. 5: Average harvested energy comparison (linear versus non-linear EH).



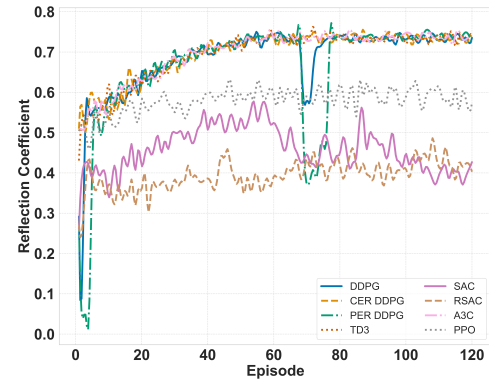
(a) Linear EH model



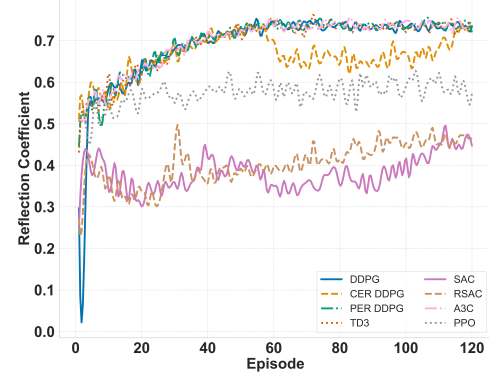
(b) Non-linear EH model

Fig. 4: Harvested energy per episode under (a) linear and (b) non-linear EH models.

(Fig. 4a), harvested energy levels generally stabilize within the 10^{-4} J range, exhibiting fluctuations dependent on the specific agent and episode. Employing the non-linear EH model (Fig. 4b) results in substantially lower harvested energy, typically fluctuating within the 10^{-8} J range. Fig. 5 further clarifies this comparison by plotting the average harvested energy across agents versus the training episode for both models. These results quantitatively demonstrate that the idealized linear EH model leads to a significant overestimation of harvested energy compared to the more realistic non-linear model.



(a) Linear EH model



(b) Non-linear EH model

Fig. 6: Γ adaptation per episode under (a) linear and (b) non-linear EH models.

3) Reflection Coefficient (Γ) Analysis: Fig. 6 illustrates the evolution of Γ per episode for the different RL agents under both linear (Fig. 6a) and non-linear (Fig. 6b) EH models. The converged values vary across algorithms, with DDPG variants, TD3, and A3C generally stabilizing at higher values ($\Gamma \approx 0.6\text{--}0.7$), while SAC and RSAC converge to lower values ($\Gamma \approx 0.4\text{--}0.5$), reflecting differences in their learned policies. Notably, the convergence patterns and the relative performance hierarchy among algorithms appear broadly similar across both the linear and non-linear EH scenarios.

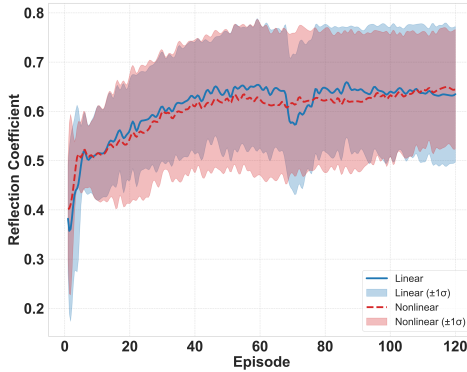


Fig. 7: Average Γ comparison (linear versus non-linear EH).

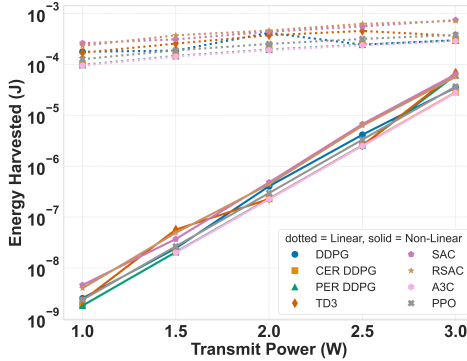


Fig. 8: Harvested energy versus transmission power under non-linear and linear EH models.

Fig. 7 provides a clearer view of the overall trend by comparing the average Γ (averaged across agents) for the linear and non-linear EH models. The average Γ converges rapidly for both cases, stabilizing around a value of approximately 0.6. This shows consistent convergence behaviors across EH models, reinforcing that effective adaptation strategies are learned independent of the underlying EH model.

4) Impact of Transmission Power on Harvested Energy: Fig. 8 depicts the harvested energy by the BN as a function of the transmission power of primary devices under the non-linear and linear EH models. Under the non-linear EH model, the harvested energy exponentially increases with transmission power. Conversely, the linear EH model assumes a direct proportionality between the harvested energy and the transmission power of the PDs, resulting in a consistently linear increase with transmission power which clearly demonstrates that linear EH model is idealized and not practically realistic.

VI. CONCLUSION

This paper addressed the data rate optimization challenge for a passive BN in a CR-NOMA BackCom network by incorporating a practical non-linear EH model and comparing eight DRL algorithms for reflection coefficient optimization. Our results revealed that while the non-linear EH model's saturation effects generally resulted in lower harvested energy compared to idealized linear models, the DRL algorithms successfully adapted their strategies to maintain robust performance. DDPG

variants (particularly CER-DDPG) and off-policy methods like SAC and TD3 demonstrated superior performance, achieving high data rates under both EH models. These findings not only show the importance of using realistic EH models in BackCom system design but also provide practical guidance for algorithm selection in energy-constrained IoT networks, laying groundwork for future extensions into multi-node scenarios and adaptive learning approaches.

ACKNOWLEDGMENT

The first three authors contributed equally to this paper. The work of H. Jung was supported by the Korea government in part under the National Research Foundation of Korea grants (NRF-2022R1A4A3033401, NRF-2022R1F1A1065367, NRF-2021M2A2A2061357) and in part under the ITRC support programs (IITP-2023-2021-0-02046) and in part under the Convergence security core talent training business support program (IITP-2023-RS-2023-00266615) supervised by the IITP.

REFERENCES

- [1] W. Liu, K. Huang, X. Zhou, and S. Durrani, "Next generation backscatter communication: systems, techniques, and applications," *EURASIP Journal on Wireless Communications and Networking*, vol. 2019, no. 1, pp. 1–11, 2019.
- [2] D. Niyato, D. I. Kim, M. Maso, and Z. Han, "Wireless powered communication networks: Research directions and technological approaches," *IEEE Wireless Communications*, vol. 24, no. 6, pp. 88–97, 2017.
- [3] N. Van Huynh, D. T. Hoang, X. Lu, D. Niyato, P. Wang, and D. I. Kim, "Ambient backscatter communications: A contemporary survey," *IEEE Communications Surveys & Tutorials*, vol. 20, no. 4, pp. 2889–2922, 2018.
- [4] F. Jameel *et al.*, "NOMA-enabled backscatter communications: Toward battery-free IoT networks," *IEEE Internet of Things Magazine*, vol. 3, no. 4, pp. 95–101, 2020.
- [5] S. Zeb, Q. Abbas, *et al.*, "NOMA enhanced backscatter communication for green IoT networks," in *16th International Symposium on Wireless Communication Systems*, pp. 640–644, 2019.
- [6] S. Asad Ullah, M. Abdullah Sohail, H. Jung, M. Omer Bin Saeed, and S. Ali Hassan, "Sum rate maximization in IoT networks with diversity-enhanced energy harvesting: A DRL-guided approach," in *IEEE Internet of Things Journal*, vol. 11, no. 18, pp. 30309–30322, Sept. 15, 2024.
- [7] H. M. Ali Zeeshan, S. A. Ullah, S. A. Hassan, Z. Ding and H. Jung, "DDPG-based Sum Rate Optimization for Opportunistic Backscatter NOMA Networks," in *IEEE Global Communications Conference*, pp. 3312–3317, 2023.
- [8] A. A. Mohammed, M. W. Baig, M. A. Sohail, S. A. Ullah, H. Jung and S. A. Hassan, "Navigating Boundaries in Quantifying Robustness: A DRL Expedition for Non-Linear Energy Harvesting IoT Networks," in *IEEE Communications Letters*, vol. 28, no. 10, pp. 2447–2451, 2024.
- [9] M. Babaei, Ü. Aygöülü, M. Başaran, and L. Durak-Ata, "BER performance of full-duplex cognitive radio network with nonlinear energy harvesting," *IEEE Transactions on Green Communications and Networking*, vol. 4, no. 2, pp. 448–460, Apr. 2020.
- [10] Y. Wang, Y. Wu, F. Zhou, Z. Chu, and Y. Wu, "Multi-objective resource allocation in a NOMA cognitive radio network with a practical non-linear energy harvesting model," *IEEE Access*, vol. 5, pp. 27838–27849, Dec. 2017.
- [11] Y. Nie, J. Zhao, J. Liu, J. Jiang, and R. Ding, "Energy-efficient UAV trajectory design for backscatter communication: A deep reinforcement learning approach," *China Communications*, vol. 17, no. 10, pp. 129–141, Oct. 2020.
- [12] T. T. Anh, N. C. Luong, D. Niyato, Y.-C. Liang, and D. I. Kim, "Deep reinforcement learning for time scheduling in RF-powered backscatter cognitive radio networks," in *Proc. IEEE WCNC*, 2018, pp. 1–6.